

RSC Advances



This is an *Accepted Manuscript*, which has been through the Royal Society of Chemistry peer review process and has been accepted for publication.

Accepted Manuscripts are published online shortly after acceptance, before technical editing, formatting and proof reading. Using this free service, authors can make their results available to the community, in citable form, before we publish the edited article. This *Accepted Manuscript* will be replaced by the edited, formatted and paginated article as soon as this is available.

You can find more information about *Accepted Manuscripts* in the [Information for Authors](#).

Please note that technical editing may introduce minor changes to the text and/or graphics, which may alter content. The journal's standard [Terms & Conditions](#) and the [Ethical guidelines](#) still apply. In no event shall the Royal Society of Chemistry be held responsible for any errors or omissions in this *Accepted Manuscript* or any consequences arising from the use of any information it contains.



Journal Name

ARTICLE

Resonance Rayleigh Scattering Detection of Heparin with Concanavalin A

Received 00th January 20xx,
Accepted 00th January 20xx

Shuguang Yan^a, Yurong Tang^{b†}, Mengling Yu^b

DOI: 10.1039/x0xx00000x

www.rsc.org/

Herein we developed a highly sensitive methodology for heparin detection based on a resonance Rayleigh scattering (RRS) spectral assay. Heparin and Concanavalin A (ConA) densely stacked together and formed nanoparticles or a well-defined brick-and-mortar nanostructure. A strong electrostatic attraction, hydrogen bond and the solid-liquid interface induced RRS enhancement. The result of absorption of spectra and TEM testified that the introduction of heparin indeed changed the structure of ConA and formed brick-and-mortar nanostructures. The optimum reaction conditions of the method and the reasons of RRS enhancement were also discussed. Combined with an RRS spectral assay, an effective biosensor has been developed for heparin. The bioassay allows sensitive detection of heparin with a detection limit of 2.48 ng/mL (3σ), a linear range from 8.28 ng/mL to 2.5 μ g/mL. The method was successfully applied to the determination of heparin in heparin sodium injection samples.

Introduction

Heparin is a highly negative charged sulfated polysaccharide with a heterogeneous mixture of diverse chains with different lengths that consist of repeated copolymers of 1-4 linked iduronic acid and glucosamine residues in a semirandom order¹. This polysaccharide plays an important role in biological systems, and interacts with a wide range of protein targets^{2,3}. Heparin has been widely used as an anticoagulant during cardiovascular surgery or used to avoid thrombosis⁴. However, heparin overdose can induce some adverse effects (such as hemorrhages and thrombocytopenia)⁵. Beyond the need for simple and ideally real-time continuous measurements of heparin levels in serum during such surgery and postoperative therapy period, there is also a desire for detection methods that can monitor the levels of heparin within infusion solutions to avoid dangerous human errors in dosing, especially for pediatric patients⁶. Thus, monitoring the amount of heparin which will be used during the surgery and the anticoagulant therapy is of crucial significance. Traditional clinical procedures for heparin detection rely on the measurements of the activated clotting time or activated partial thromboplastin time⁷. These methods are not sufficiently reliable and accurate for clinical settings because of their lack of specificity and potential interference from other factors⁸. Thus, many researchers have attempted to develop new methods for the detection of heparin, including fluorimetry⁹, phosphorimetry¹⁰, colorimetry¹¹, light scattering¹² and electrochemical

methods¹³. However, such approaches are either well-selected or cost-efficient but poorly-sensitive and expensive. Furthermore, con A often has poor toxicity profiles¹⁴. The limitations of previous approaches to protamine replacement therapy¹⁵ encouraged us to explore an innovative self-assembling approach to multivalent heparin binding.

The effect of heparin on protein aggregation would appear from the literature to comprise both promotion and inhibition. These conflicting results could reflect the problem of comparing different proteins with different levels of heparin affinity and different aggregation mechanisms¹⁶ which depend on solution pH and ionic strength¹⁷. Protein aggregation could promote formation and interpretation of heparin effects, because protein surface is better conserved and formation of unfolded states is minimized. Protein aggregation is controlled by electrostatics, and the protein surface charge anisotropy regulates protein self-association mechanisms. Electrostatics also control heparin-protein binding. There is a need to explain the possible linkage between electrostatically driven aggregation and heparin-protein binding.

RRS has been known for its sensitivity and simplicity as an analytical technique developed in recent years¹⁸. This technique has been applied successfully to study macromolecules^{19,20}. RRS is very sensitive to the interaction caused by weak binding forces such as van der Waals interaction force, hydrophobic interaction, and aggregation interaction of biological macromolecules²¹. The spectral characteristics and RRS intensity may provide helpful new information to the study of the interaction of biological macromolecules and the molecular recognition²². Nevertheless, a sensitive, reliable and easily operated detection method for heparin is still expected. Few works, so far, has been reported regarding the foundation of RRS-based protocols to directly detect heparin utilizing protein.

In this paper, the development of novel RRS sensors for the detection of biomolecular specific interactions based on the interaction between heparin and ConA was reported.

^aCollege of Energy Resources, Chengdu University of Technology, Chengdu 610059, China

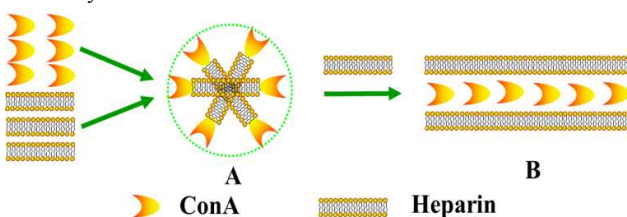
^bCollege of Material and Chemistry & Chemical Engineering, Chengdu University of Technology, Chengdu 610059, China

† Corresponding author. Tel. & fax: +862884079009. E-mail address:

tangyurong@163.com

DOI: 10.1039/x0xx00000x

Different combination modes were controlled via the concentration of heparin binding ConA in water solutions was firstly assembled. Heparin and ConA bind densely together to form nanoparticles and a well-defined brick-and-mortar nanostructure (scheme 1). A strong electrostatic attraction, hydrogen bond and the solid-liquid interface induce RRS enhancement. To the best of our knowledge, it is the first time that selective binding of ConA to heparin has been detected by means of RRS using nanostructured sensors. Therefore, the objective of this study was to develop a facile RRS bioassay for sensitive and selective detection of heparin in biological fluids via a strategy of the target-involved assembly of ConA.



Scheme 1 Stepwise macromolecular interactions observed between a ConA and heparin, which are accompanied by RRS changes.

Experimental

Materials and reagents

ConA was purchased from sigma-Aldrich (shanghai) trading Co. Led. Heparin sodium purchased from Aladdin (Shanghai, China) has 185 USP units/mg. Britton-Robinson buffer solution (BR) was used to control the acidity of the aqueous medium. All the reagents were used for analytical reagent grade without further purification and deionized water with conductivity of $18.24 \text{ M}\Omega\text{cm}^{-1}$ was used in this experiment from a water purification system (ULUPURE, Chengdu, China).

Instruments

Transmission electron microscopy (TEM) of heparin-ConA complex was carried out on a Tecnai G2 F20 S-TWIN transmission electron microscope at an accelerating voltage of 200 kV (FEI Co., America). Samples were prepared for analysis by evaporating a drop of aqueous product on a lacey carbon copper TEM grid. The UV-vis spectra and RRS spectra were obtained with a U-2910 UV-vis spectrophotometer and an F-7000 fluorescence spectrophotometer (Hitachi Co., Tokyo, Japan).

Experimental procedure

22.5 $\mu\text{g}/\text{mL}$ ConA, 150 μL BR (pH=4.56) and appropriate amounts of heparin were added into a 2 mL colorimetric tube, then diluted with deionized water to the mark and mixed thoroughly with gentle shake. After incubated for 10 min, the RRS and UV-vis spectra of solution were examined.

Results and discussion

Nanoparticles assembled by heparin binding ConA

To study the interaction between the ConA and heparin, a varying concentration of the heparin was added to 22.5 $\mu\text{g}/\text{mL}$ of ConA solution, and the RRS intensity at 294 nm was recorded. As shown in Fig. 1a, the RRS intensity was obviously enhanced with the increasing concentration of

heparin, and it reached a maximum of 2.5 $\mu\text{g}/\text{mL}$ of the heparin in ConA solution. The great enhancement of RRS intensity indicated that ConA had interacted with heparin to assemble heparin-ConA nanoparticles. The process of nanoparticles aggregation is presented in Scheme 1A.

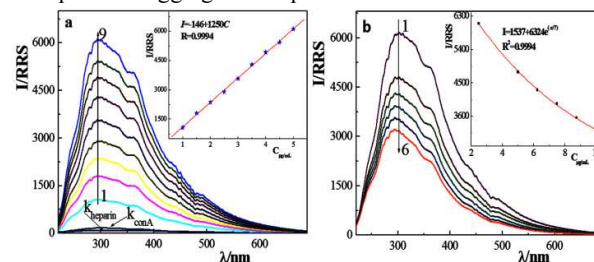
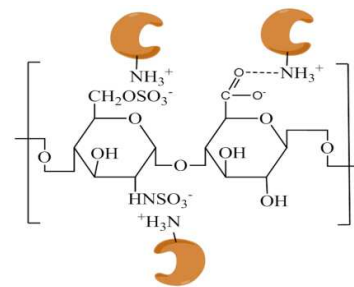


Figure 1 (a) RRS spectra of conA-heparin system. Concentration of conA 22.5 $\mu\text{g}/\text{mL}$; concentration of heparin 1-9 ($\mu\text{g}/\text{mL}$): 0.5, 0.75, 1.0, 1.25, 1.5, 1.75, 2.0, 2.25, 2.5, respectively. Inset of (a) showed linear plots of the RRS at 294 nm against the concentration of heparin. (b) RRS spectra of conA-heparin system. Concentration of conA 22.5 $\mu\text{g}/\text{mL}$; concentration of heparin 1-6 ($\mu\text{g}/\text{mL}$): 2.5, 5, 6.25, 7.5, 8.75, 10, respectively. Inset of (b) showed nonlinear plots of the RRS at 294 nm against the concentration of heparin.

However, when the concentration of heparin changed from 2.5 $\mu\text{g}/\text{mL}$ to 10 $\mu\text{g}/\text{mL}$, the RRS intensity of the ConA solution was obviously reduced with the increasing concentration of heparin (Fig.1b). We propose that heparin, as a relatively inflexible polymer, organizes ConA aggregating along its backbone as a consequence of electrostatic interactions, which interacted with heparin to assemble a well-defined brick-and-mortar nanostructure²³, and then the volume of the scattering nanostructures reduced and the solid-liquid interface disappeared, which produced reduced scattering and reduced the scattering intensities. The process of brick-and-mortar aggregation is presented in Scheme 1B. Under the condition of weak acid, heparin carries negative charges, and can bind to the ConA through the electrostatic attraction between its negative charges and the positive charges of the amino in ConA (scheme 2). Thus some of them will aggregate each other to form a brick-and-mortar nanostructure. Therefore, it is highly feasible to assemble nanoparticles using electropositive ConA and heparin with dense negative charges.

Scheme 2 Schematic diagram of the model of the electrostatic



attraction and hydrogen bond between conA and heparin.

The interaction between ConA and some other mucopolysaccharide (chondroitin sulfate and sodium hyaluronate) were also investigated. The two types of the mucopolysaccharide contain the same backbone and the difference among them lies in their substituent moieties (Fig.2a, 2b). As shown in Fig.2c, 2d, the RRS intensities appear to be related to the substituent moieties of mucopolysaccharide. Chondroitin sulfate has less negative charges and less sulfonic acid group than heparin, which

would lead to instability in the aggregation of nanoparticles. In particular, sodium hyaluronate has no sulfonic acid group, so the binding site for ConA is less than other mucopolysaccharide. Therefore, sufficient charges are critical to aggregate nanoparticles when mucopolysaccharide are binding ConA. Regarding these two special features, heparin may be the most suitable mucopolysaccharide for assembling brick-and-mortar nanostructure.

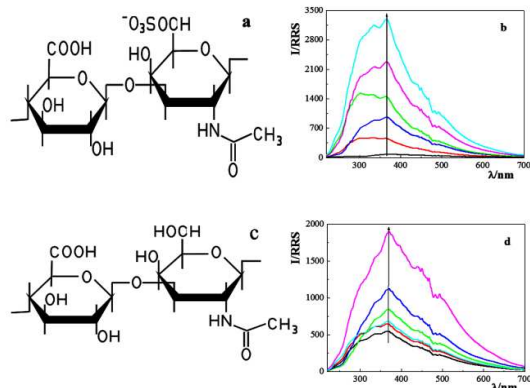


Figure 2 (a) Chemical structure of chondroitin sulfate A sodium in this study. (b) RRS spectra of conA-chondroitin sulfate A sodium system. Concentration of conA 22.5 μg/mL; concentration of chondroitin sulfate A sodium 1-6 (μg/mL): 5, 10, 15, 20, 25, 30, respectively. (c) Chemical structure of sodium hyaluronate in this study. (d) RRS spectra of conA-sodium hyaluronate system. Concentration of conA 22.5 μg/mL; concentration of sodium hyaluronate 1-6 (μg/mL): 5, 10, 15, 20, 25, 30, respectively.

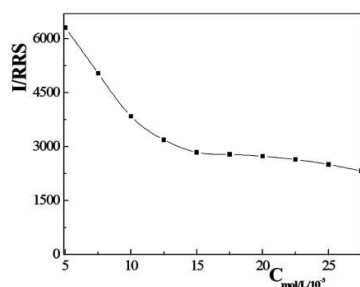


Figure 3 RRS intensities of conA solutions treated with heparin under different ionic strengths. Concentration of conA: 22.5 μg/mL, heparin: 2.5 μg/mL, BR 150 μL, pH=4.56. Concentration of NaCl (10⁻³ mol/L): 5, 7.5, 10, 12.5, 15, 17.5, 20, 22.5, 25, 27.5, respectively.

The electrostatic attraction between ConA and heparin plays a significant role in the aggregation of nanoparticles. In general, the electrostatic attraction is associated with the ionic strength of the solution. Herein, varying concentrations of NaCl were added to ConA to control their ionic strength during the binding of nanostructures. As shown in Fig. 3, the RRS intensity decreased gradually with increasing ionic strength of the media, and it attained the minimum at the highest ionic strength. Besides, under the optimal condition, heparin carries negative charges and ConA carries positive charges. It can be demonstrated that the electrostatic attraction between the heparin and ConA is neutralized after the binding of heparin and ConA. Furthermore, the RRS intensity decreased hardly when the excess NaCl was added. The result indicated that in addition electrostatic attraction

between the heparin and ConA, hydrogen bond may be formed.

TEM analysis of nanoparticles

The RRS intensity is associated with the nanoparticle size of colloid solution. Herein, the size of the nanoparticles was investigated by TEM, and the result is shown in Fig. 4. At lower concentrations of heparin (lower than 2.5 μg/mL), the diameter of the nanoparticles was close to 300 nm (Fig. 4a). With the increasing number of heparin (2.5 μg/mL-10 μg/mL), the structure of the nanoparticle aggregation transformed to brick-and-mortar aggregation (Fig. 4b).

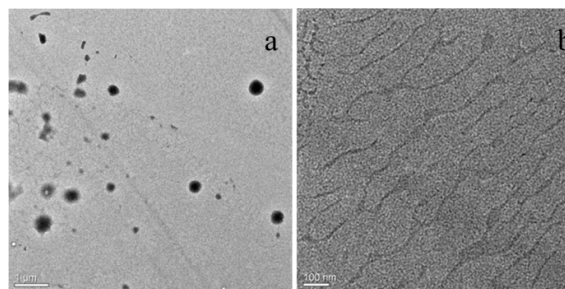


Figure 4 (a) TEM image of conA-heparin complex in low concentration of heparin (2.5 μg/mL). (b) TEM image of conA-heparin complex in high concentration of heparin (10 μg/mL).

The reasons for the above two opposing size-variation trends may depend on the different properties of large nanoparticles and brick-and-mortar nanostructures. The large nanoparticles were assembled at lower concentration of heparin, where a large number of ConA molecules or its micelle structure might be absorbed by a single heparin molecule. The whole large nanoparticle was loose and full of holes due to the electrostatic repulsion of ConA molecules. In the case of higher concentration of heparin, because heparin contains many carboxyl groups (-COO⁻) and the -NH₃⁺ of ConA in aqueous solution, it shortens the distance of the neighboring heparin and ConA, and compacts the whole nanoparticle through strong hydrogen bonds between the -COO⁻ of heparin and -NH₃⁺ of ConA. In this case, the hydrogen bonds would play an important role in maintaining the brick-and-mortar nanostructure.

The Reasons for the enhancement and reducing of RRS in low concentration of heparin

Generally, the RRS intensity depends largely on the size of particles under the same experimental conditions. Therefore, it can be indicated that the variation of RRS intensity in solution was probably ascribed to the size alteration of nanoparticles caused by heparin. As for the enhancement mechanism, in theory, RRS enhancing in this system could occur by:

Resonance enhanced Rayleigh scattering effect RRS was an absorption re-scattering process produced by the resonance between the Rayleigh scattering and the light absorption with the same frequency when the wavelength of Rayleigh scattering was located at its absorption band²⁴. Therefore, RRS spectrum was closely related to the absorption spectrum. From the comparison of RRS spectrum of the heparin-ConA complex with its absorption spectrum, from Fig. 5 it can be seen that the RRS peak at 294 nm were close to the absorption band, which would result in the resonance enhanced scattering.

Increase of the molecular volume It is well known that the increase of the volume of the scattering molecule was

advantageous to the enhancement of scattering intensity²⁵. Heparin carries negative charges while ConA carries positive charges. Heparin and ConA aggregation was formed through electrostatic attraction and hydrogen bond, which resulted in the increase of the diameter up to about 300-500 nm. Thus, the increase of the molecular volume was one of the reasons for the RRS enhancements. It was proved by the TEM image of Fig. 4. The way how the ConA attached to heparin was shown in scheme 2.

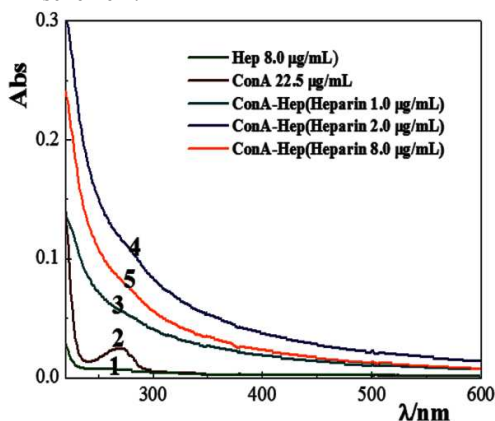


Figure 5 UV-vis spectra of (1) heparin (1.0 $\mu\text{g}/\text{mL}$), (2) conA (22.5 $\mu\text{g}/\text{mL}$), (3), (4) and (5) conA in the presence of heparin (conA as reference). BR 150 μL , pH=4.56, conA 22.5 $\mu\text{g}/\text{mL}$, heparin, 1.0, 2.0, 8.0 $\mu\text{g}/\text{mL}$, respectively.

Formation of solid-liquid interface When heparin binds ConA to form binding products, most of their electric charges were neutralized, which cause the increase of the hydrophobicity of the binding products, the liquid-solid interface between then nanoparticles and water may be formed²⁶, which produces surface enhanced scattering and enhances the scattering intensities.

Change of the conformation of the protein Proteins are stable spherical and small in the aqueous, so the scattering of the proteins are weak, however, when the carbonyl (C=O) of the peptide chain of proteins bind with $-\text{COO}^-$ on the surface of a heparin by hydrogen bonds, the original regular and repeating secondary structure of the protein held together by a peptide chain and a hydrogen bond was destroyed and the structure became extended and loose^{27,28}, which was similar to the denaturing of the protein. This can enhance the scattering.

Optimization of general procedure

The influence of buffer solution on the RRS intensity of the system was investigated, such as SCBS, BR and PBS. The results indicated that BR was the best buffer solution of the reaction system. Therefore, in this case, we used the BR of pH 3.29 to 5.72 to investigate the effect of pH on the RRS intensity (Fig. 6a). RRS intensity reached the maximum and remained stable when the pH range was 4-5. The selected pH was 4.56. The most suitable volume of BR buffer solution for the reaction of ConA with heparin was 150 μL . (Fig. 6b). The effect of ConA concentration on the RRS intensity of the system was investigated. The system had the most suitable sensitivity and the system was stable when the concentration of ConA was 22.5 $\mu\text{g}/\text{mL}$ for the system (Fig. 6c). Therefore, the concentration of ConA 22.5 $\mu\text{g}/\text{mL}$ was suitable. We investigated the factors of reaction time influencing the RRS of the system. The RRS of ConA increased quickly in the presence of heparin, and reached stability in 10 min.

Therefore, 10 min was chosen for further experiments (Fig. 6d).

Sensitivity and selectivity

Under the optimum conditions, the RRS intensities of the system are determined at the maximum scattering wavelength. As indicated in Fig. 1a, the RRS of the ConA is sensitive to heparin and linearly increase with the concentration of heparin from 8.28 ng/mL to 2.5 $\mu\text{g}/\text{mL}$ and the limit of detection is 2.48 ng/mL (3σ). The linear regression equation is $I = 2500C - 146$ (where C is the concentration of heparin, $\mu\text{g}/\text{mL}$). The relative standard deviation (RSD) for eleven replicate detections is 2.07%. It can be seen that this method has a low detection limit and will be a valuable tool for the determination of heparin.

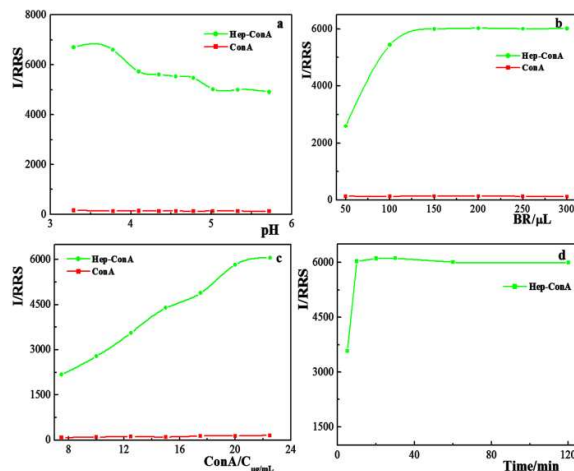


Figure 6 (a) The effect of pH on RRS intensities. conA, 22.5 $\mu\text{g}/\text{mL}$, BR 150 μL , heparin, 2.5 $\mu\text{g}/\text{mL}$. (b) The effect of amount of BR on RRS intensities. conA, 22.5 $\mu\text{g}/\text{mL}$, heparin, 2.5 $\mu\text{g}/\text{mL}$. (c) The effect of conA concentration on RRS intensities. BR 150 μL , pH=4.56, heparin 2.5 $\mu\text{g}/\text{mL}$. (d) The time-dependent RRS of the system after addition of heparin. conA, 22.5 $\mu\text{g}/\text{mL}$, BR 150 μL , pH=4.56, heparin, 2.5 $\mu\text{g}/\text{mL}$.

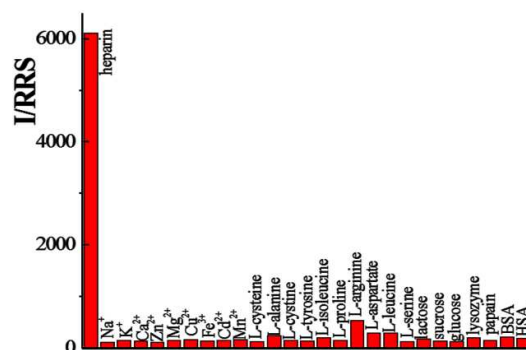


Figure 7 Selectivity of conA probe towards heparin. conA, 22.5 $\mu\text{g}/\text{mL}$, BR 150 μL , pH=4.56, heparin, 2.5 $\mu\text{g}/\text{mL}$. The concentration of Na^+ 0.5 mmol/L, K^+ 0.5 mol/L, Ca^{2+} 0.5 mmol/L, Zn^{2+} 5 mmol/L, Mg^{2+} 0.5 mmol/L, Cu^{2+} 5 mmol/L, Fe^{3+} 2.5 mmol/L, Cd^{2+} 2.5 mmol/L, Mn^{2+} 0.25 mmol/L. L-cysteine, L-alanine, L-cystine, L-tyrosine, L-isoleucine, L-proline, L-arginine, L-aspartate, L-leucine, L-serine, 5 mmol/L, respectively. actose, sucrose, glucose 2.5 mmol/L, respectively. lysozyme: 120 $\mu\text{g}/\text{mL}$, papain: 340 $\mu\text{g}/\text{mL}$, BSA: 120 $\mu\text{g}/\text{mL}$, HSA: 100 $\mu\text{g}/\text{mL}$.

Study on the RRS response of the ConA to various analytes shows good selectivity of the present assay for heparin. As shown in Fig. 7, only heparin causes a significant

Journal Name ARTICLE

increase in relative RRS intensity of ConA, while other species have no evident effect on the RRS intensities. The results demonstrate that physiological levels of cation, amino acid and small biomolecules do not interfere with the detection. Specially, large molecules such as lysozyme, papain, BSA and HSA level of 120 µg/mL, 340 µg/mL, 120 µg/mL, 100 µg/mL respectively do not interfere with the detection.

Application in heparin sodium injection samples

To test the proposed assay, this method was applied to determine heparin in heparin sodium injection samples. A 5 µL portion of heparin sodium injectable was pipetted into a 10-mL calibrated flask and was diluted to the mark with water. A 10 µL portion of this solution of heparin was pipetted into a 20-mL volumetric flask, and then diluted to the mark with water. A 20 µL portion of this solution of heparin was pipetted into a 40-mL volumetric flask, and then diluted to the mark with water. The following procedures are same with the above. The results and recoveries are listed in Tables 1. The recoveries were between 97.0% and 101%. Therefore, the method can be applied to the determination of heparin in heparin sodium injection with satisfactory results.

Table 1 Results of recoveries of heparin in heparin sodium injection samples.

Sample	Found (µg/mL, n=5)	Added (µg/mL)	Total found (µg/mL, n=5)	Recovery %
1	1.901	2	3.894	97
2	1.941	2	3.927	98
3	2.022	2	4.047	101

Conclusions

In summary, we have developed a convenient ConA-based detection system for heparin. UV-vis, RRS and TEM indicate that binding to heparin induces nanoscale organization. The large nanoparticles were assembled by lower concentrations of ConA and heparin molecules, while the brick-and-mortar nanostructure were constructed under higher concentration of heparin due to electrostatic repulsion among heparin and their hydrogen bonds binding to ConA molecules. Such simple materials may be potentially used in biomedical applications. In future work, the ability of this heparin binding protein to intervene in biological processes will be further investigated, as will higher-generation dendritic systems and the potential of these systems to degrade and disaggregate, thus leading to controlled heparin binding and released protein.

Acknowledgements

This work was supported by the National Natural Science Foundation of China (Nos. 21375089 and 21105068). The authors would like to show gratitude for Dr. Shanling Wang at Analytical & Testing Center of Sichuan University for her assistance in the TEM analysis.

Notes and references

The authors declare no competing financial interest.

1. D. L. Rabenstein, *Nat. Prod. Rep.* 2002, 19, 312-331.
2. I. Capila, R.J. Linhardt, *Angew. Chem. Int. Ed.* 41(2002)390-412.

3. A.C. Rodrigo, A. Barnard, J. Cooper, D.K. Smith, *Angew. Chem. Int. Ed.* 50(2011)4675-4679.
4. N. Mackman, Triggers, *Nature*, 451(2008)914-917.
5. T.E. Warkentin, M.N. Levine, J. Hirsh, P. Horsewood, R.S. Roberts, M. Gent, J.G. Kelton, *New Engl. J. Med.* 332(1995)1330-1336.
6. R. Cao, B.X. Li, *Chem. Commun.* 47(2011)2865-2867.
7. P.D. Raymond, M.J. Ray, S.N. Callen, N.A. Marsh, *Perfusion* 18(2003)269-271.
8. M.N. Levine, J. Hirsh, M. Gent, A.G. Turpie, M. Cruickshank, J. Weitz, D. Anderson, M. Johnson, *Arch. Intern. Med.* 154(1994)22-24.
9. M. Wang, D.Q. Zhang, G.X. Zhang, D.B. Zhu, *Chem. Commun.* 37(2008)4469-4471.
10. H. Yan, H.F. Wang, *Anal. Chem.* 83 (2011) 8589-8595
11. T. Briza, Z. Kejik, I. Cisarova, J. Kralova, P. Martasek, V. Kral, *Chem. Commun.* 16(2008) 1901-1903.
12. S.P. Liu, H.Q. Luo, N.B. Li, Z.F. Liu, W.X. Zheng, *Anal. Chem.* 73(2001)3907-3914.
13. K.L. Gemene, M.E. Meyerhoff, *Anal. Chem.* 82(2010)1612-1615.
14. T.R. Silvers, J.K. Myers, *Biochemistry* 52(2013)9367-9374.
15. S.M. Bromfield, P. Posocco, C.W. Chan, M. Calderon, S.E. Guimond, J.E. Turnbull, S. Priel, D.K. Smith, *Chem. Sci.* 5(2014)1484-1492.
16. Y.S. Cho, K.H. Ahn, *J. Mater. Chem. B* 1(2013)1182-1189.
17. B.B. Minsky, B.Q. Zheng, P.L. Dubin, *Langmuir* 30(2014)278-287.
18. Y. Shi, H.Q. Luo, N.B. Li, *Chem. Commun.* 49(2013)6209-6211.
19. W.W. Song, N.B. Li, H.Q. Luo, *Anal. Biochem.* 422(2012)1-6.
20. Y.R. Tang, Y. Zhang, Y.Y. Su and Y. Lv, *Talanta*, 115(2013)830-836.
21. L. Kong, Z. F. Liu, X.L. Hu, S. P. Liu, J. D. Meng, *Journal of Luminescence*, 137(2013)186-190.
22. P. P. Li, S. P. Liu, S. G. Yan, X. Q. Fan, Y. Q. He, *Colloids Surf. A: Physicochem. Eng. Aspects* 392(2011)7-15.
23. A.T. Wright, Z.L. Zhong, E.V. Anslyn, *Angew. Chem. Int. Ed.* 44(2005)5679-5682.
24. S.P. Liu, F. Wang, Z.F. Liu, X.L. Hu, A.R. Yi, H. Duan, *Anal. Chim. Acta* 601 (2007)101-107.
25. Q.Y. Xu, Z.F. Liu, X.L. Hu, L. Kong, S.P. Liu, *Anal. Chim. Acta* 707 (2011) 114-120.
26. J.J. Peng, S.P. Liu, L. Wang, Z.W. Liu, Y.Q. He, *J. Colloid Interf. Sci.* 338 (2009) 578-583.
27. S.P. Liu, Z. Yang, Z.F. Liu, L. Kong, *Anal. Biochem.* 353(2006)108-116.
28. J.J. Peng, S.P. Liu, S.G. Yan, X.Q. Fan, Y.Q. He, *Colloids Surf. A: Physicochem. Eng. Aspects* 359 (2010) 13-17.